

# Magneto-optical study of excitonic states in $\text{In}_{0.045}\text{Ga}_{0.955}\text{As}/\text{GaAs}$ multiple coupled quantum wells

T. Wang,\* M. Bayer, A. Forchel, N. A. Gippius, and V. Kulakovskii  
*Technische Physik, Universität Würzburg, Am Hubland, D-97074 Würzburg, Germany*  
 (Received 14 September 1999; revised manuscript received 14 April 2000)

The excitonic states have been investigated in  $\text{In}_{0.045}\text{Ga}_{0.955}\text{As}/\text{GaAs}$  heterostructures consisting of  $i$  quantum wells ( $i=1,2,3,4$ ) with 7.5 nm well thickness. For a 2.5 nm barrier thickness between the wells, the electronic states are strongly coupled. Because of the coupling, the heavy-hole exciton  $n\text{shh}$  of each single quantum well is split into  $i^2$  states. The states can be characterized according to their symmetry under a combination of the reflections of the single particles at the quantum-well plane. The energy order of the symmetric and antisymmetric states as a function of quantum-well number is investigated in detail, and compares well to the theoretical calculation. These coupled quantum-well structures exhibit somewhat three-dimensional character based on the study of their exciton binding energies and wave functions. Highly resolved photoluminescence excitation spectra are presented, measured in magnetic fields up to 13 T using circularly polarized light. Strong mixing between light- and heavy-hole excitons causes optical transitions into high-angular-momentum exciton states and strong anticrossing effects. An anticrossing between the  $3d\text{hh}_{11}$  and  $\text{hh}_{21}$  exciton is observed. Also, the light-hole exciton is found to possess  $\Gamma_{7g}$  and  $\Gamma_{6g}$  symmetries.

## I. INTRODUCTION

Investigation of excitonic states in semiconductor quantum wells is of considerable interest; it can provide us with much information on excitonic properties.<sup>1-25</sup> In particular, excitons in the presence of a magnetic or electrical field are of special interest. The external field enhances the exciton oscillator strength, which leads to the appearance of more excitonic transitions, including excited excitonic states. Also, interactions between excitons can be observed in high magnetic field. The observation of excited excitonic states can provide information on the exciton binding energy,<sup>15,18,19</sup> the interaction between excitons shows the symmetries of exciton states,<sup>1,13</sup> and the appearance of forbidden transitions indicates the mixing effect of the valence-band structure.<sup>3,4,15,17,19,22-25</sup> Theoretically, excitons or excitons in an external field have been studied in detail by Bauer and Ando,<sup>1,2</sup> Yang and Sham,<sup>14</sup> and Chan.<sup>5</sup> However, most of this work concentrates on single-quantum-well structures, in particular,  $\text{GaAs}/\text{Al}_x\text{Ga}_{1-x}\text{As}$  single-quantum-well structures. Investigation of coupled quantum-well structures shows more interesting features. The coupling between the separated quantum wells has a strong influence on the excitonic states. Recently, the authors investigated the spin splitting of a parity-forbidden transition in a coupled double  $\text{In}_x\text{Ga}_{1-x}\text{As}/\text{GaAs}$  quantum-well structure, confirming that the appearance of this parity-forbidden transition is due to strong mixing between the heavy-hole exciton with high-angular-momentum and light-hole excitons.<sup>25</sup> So far, most studies on coupled quantum-well structures are based on coupled double-quantum-well (CDQW) structures, i.e., structures consisting of two identical single quantum wells separated by a thin barrier.<sup>6-12,16,20,25</sup> By modifying the barrier thickness, one can adjust the degree of coupling. If more quantum wells are introduced, for example, three or four, the original excitonic state in the separated quantum wells should be split into more excitonic states due to coupling, which can provide more information about the excitonic

state compared with the case of a CDQW. To our knowledge, there has been no such report until now. In this paper, structures consisting of  $i$  quantum wells ( $i=1,2,3,4$ ) separated by a thin barrier are used to study coupling effects on the excitonic state. Highly resolved photoluminescence (PL) and photoluminescence excitation (PLE) spectra of excitons in magnetic fields up to 13 T are used to study the effect of mixing between heavy- and light-hole excitons on the excitonic state, in particular, the behavior of forbidden transitions and the unusual properties of the light-hole exciton.

The paper is organized as follows. In Sec. II the investigated sample structures and experimental setup are described in detail. The investigations of the coupling effect on the single-particle state at  $B=0$  and the exciton binding energy are carried out in Secs. III and IV, respectively. Section V mainly concerns the forbidden-transition  $\text{hh}_{21}$  exciton properties and 1lh exciton symmetry due to the strong mixing between heavy- and light-hole excitons.

## II. SAMPLES AND EXPERIMENTAL SETUP

Undoped  $\text{In}_{0.045}\text{Ga}_{0.955}\text{As}/\text{GaAs}$  coupled quantum wells separated by thin GaAs spikes were grown by solid-source molecular-beam epitaxy along the [001] direction of semi-insulating (001) GaAs substrates. The growth sequence was as follows: (1) 500 nm GaAs buffer, (2) coupled quantum-well structure, and (3) 200 nm GaAs cap layer. These structures consist of  $i$  quantum wells ( $i=1,2,3,4$ ). For each separated quantum well, 7.5 nm well thickness was chosen in all samples. The thickness of the GaAs spikes between quantum wells was 9 monolayers (ML) in all cases.

The samples are mounted in a He cryostat, containing a superconducting solenoid ( $B \leq 13$  T) for the PL and PLE measurements at 4.2 K. The direction of magnetic field is parallel to the growth direction of the samples. Photoexcitation and collection of the emission were carried out using an optical fiber with a diameter of 200  $\mu\text{m}$ . A polarizer and a quarter plate were placed between the outlet of the optical

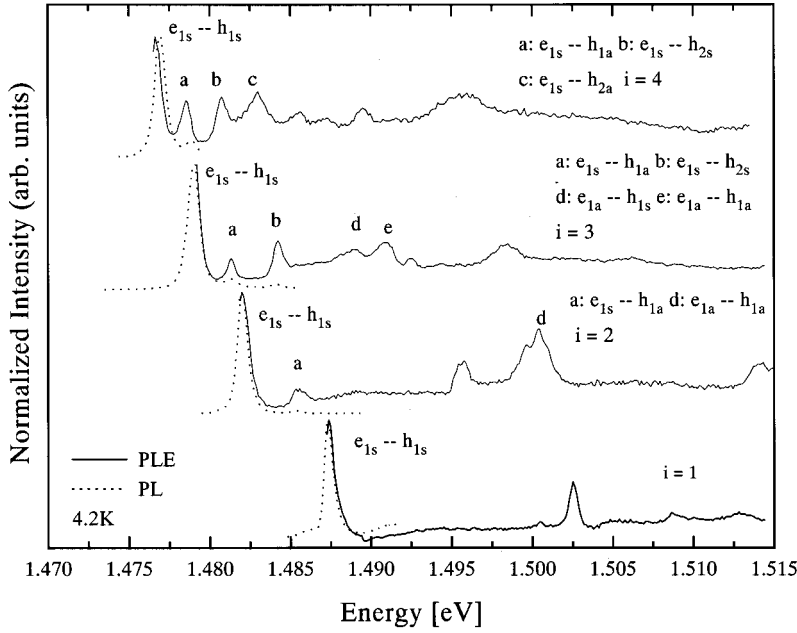


FIG. 1. PL (dotted lines) and PLE (solid lines) spectra of structures with quantum-well number  $i=1,2,3,4$  (from bottom to top).

fiber and the sample in order to record spectra in the  $\sigma^+$  and  $\sigma^-$  polarizations. For excitation, we used a Ti-sapphire laser pumped by an  $\text{Ar}^+$  laser. The luminescence was dispersed by a double monochromator with a focal length of  $f=1$  m and was detected by a Peltier-cooled GaAs photomultiplier interfaced with a photon-counting system. In order to avoid many-body effects, a low excitation power was used.

### III. SINGLE-PARTICLE STATES IN THE COUPLED QUANTUM WELLS

Figure 1 shows PL (dotted lines) and PLE (solid lines) spectra recorded at  $B=0$ . From bottom to top, the spectra of samples with quantum-well number  $i=1,2,3,4$  are displayed. A very sharp luminescence peak is from the transition between the electron and the heavy-hole ground state in each case. The linewidth is 0.55 meV for  $i=1,0.7$  meV for  $i=2,3$ , and 0.8 meV for  $i=4$ , indicating very high-quality samples. The high quality of the samples is also confirmed by the PLE excitation spectra. In all cases, the Stokes shift is below 0.2 meV.

It is very interesting to investigate the excitonic states in relation to the number of coupled quantum wells. First, we discuss the case of  $i=1$ , i.e., a single quantum well (SQW). For a SQW of 7.5 nm thickness, there is only one confined electronic state and one confined heavy-hole state in the quantum well. Because of the strain effect, the splitting of light and heavy holes is higher than the barrier potential. Thus the light hole is unconfined. The exciton envelope function can be described by the so-called hydrogenic model parameters ( $nm$ ), where  $n$  is the principal quantum number and  $m$  is the angular-momentum quantum number ( $\dots, d^-, p^-, s, p^+, d^+, \dots$ ). In the PLE spectrum of this SQW, the ground-state peak at 1.4874 eV corresponds to  $1s$  hh, which describes a simple structure with a 62:38 band offset, normally used for  $\text{In}_x\text{Ga}_{1-x}\text{As}/\text{GaAs}$  heterostructure. Consider what happens to the exciton in such a single quantum well when we introduce  $i$  identical wells at some finite separation. In order to produce a strong coupling effect, a barrier

of 2.5 nm GaAs is used to separate these quantum wells. The strong coupling lifts the degeneracy of the  $i$  states of  $i$  separated quantum wells and  $i$  subbands appear in both conduction and valence bands. Figures 2(a) and 2(b) depict the subband energy versus quantum-well number for the valence band and conduction band, respectively. Figure 2(a) indicates that the subband number in the valence band is equal to the quantum-well number. For example, in the case of  $i=4$ , there are four confined heavy-hole states. Figure 2(b) shows the case of the conduction band. The electron effective mass is much smaller than that of the heavy hole, which results in enhanced coupling for the electron. This enhanced coupling lifts the degeneracy further. The energy splitting between the subbands in the conduction band becomes larger than that in the valence band. Consequently, in the case of  $i=3$ , there exist only two confined subbands in the conduction band. In the case of  $i=4$ , only three subbands in the conduction band can be confined, as shown in Fig. 2(b). Because of the inversion symmetry of the Hamiltonian, the excitonic states should be either even (symmetric states) or odd (antisymmetric states) under the operation  $(z_e, z_h) \rightarrow (-z_e, -z_h)$ . In Fig. 2, the electron or heavy-hole states appear in order of increasing energy: the symmetric state ( $e/h_{1s}$ ), the antisymmetric state ( $e/h_{1a}$ ), the first excited symmetric state ( $e/h_{2s}$ ), the first excited antisymmetric state ( $e/h_{2a}$ ), and so on for other higher excited states.

Without considering the state parity,  $i$  subbands in the conduction and valence bands should produce  $i^2$  transitions. In a word, due to the coupling, the heavy-hole exciton  $1s$ hh of each single quantum well is split into  $i^2$ shh states. For example, in the case of  $i=2$ , there are two subbands in both conduction and valence bands as shown in Fig. 2, which should produce four states, i.e.,  $e_{1s}-h_{1s}$ ,  $e_{1s}-h_{1a}$ ,  $e_{1a}-h_{1s}$ , and  $e_{1a}-h_{1a}$ . Because the energy separation between subbands in the conduction band is much larger than that in the valence band, the states in order of increasing energy should be  $e_{1s}-h_{1s}$ ,  $e_{1s}-h_{1a}$ ,  $e_{1a}-h_{1s}$ ,  $e_{1a}-h_{1a}$ . For example, in the case of  $i=2$  in Fig. 1, the peak at 1.4800 eV is from the

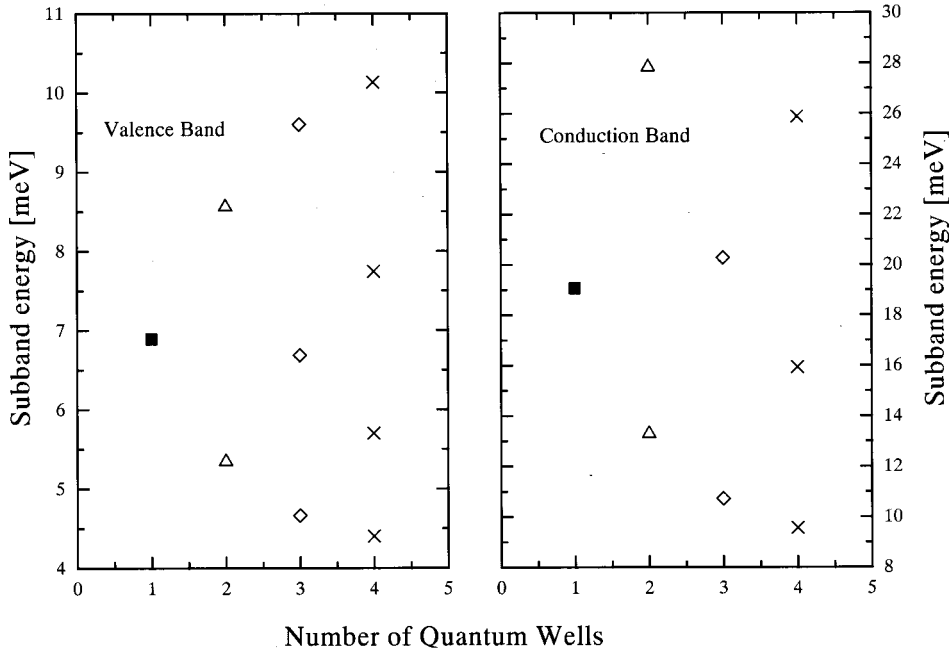


FIG. 2. Subband energy levels versus quantum-well number (a) in the valence band and (b) in the conduction band.

$e_{1s}$ - $h_{1s}$  exciton transition, and the peaks at 1.4855 and 1.5005 eV from the  $e_{1s}$ - $h_{1a}$  and  $e_{1a}$ - $h_{1a}$  exciton transitions, respectively.

In Fig. 3, the transition energy is plotted as a function of quantum-well number, using the experimental results from Fig. 1. For simplicity, we would like to concentrate on the study of excitonic transitions from  $e_{1s}$  to heavy-hole states with different subband indices. The calculation is carried out based on the single-particle model including the excitonic effect. With increasing quantum-well number, the transition energies for  $e_{1s}$ - $h_{1s}$ ,  $e_{1s}$ - $h_{1a}$ , and  $e_{1s}$ - $e_{2s}$  decrease as shown in Fig. 3. This is expected, since the subband energy for the same subband index decreases with increasing quantum-well number for both conduction and valence bands as shown in Fig. 2. Therefore, for transitions related to the  $e_{1s}$  state (i.e., in the cases of  $e_{1s}$ - $h_{1s}$ ,  $e_{1s}$ - $h_{1a}$ ,  $e_{1s}$ - $h_{2s}$ , and  $e_{1s}$ - $h_{2a}$ ), the transition energy should decrease with increasing quantum-well number, which agrees with the experimental results.

#### IV. COUPLING EFFECT ON EXCITON BINDING ENERGIES

The dependence of the exciton binding energy on quantum-well number is investigated in this section. First, we give a description of the symbols for excitonic states  $nm(hh/lh)_{n1/n2}$ , where  $n$  and  $m$  have the same meaning as in Sec. III, hh/lh means heavy/light-hole exciton, and  $n1/n2$  represents the subband index in the conduction/valence band.

The ground-state exciton binding energies  $E_B^X$  can be extracted from the transition energies. The  $2shh_{11}$ - $1shh_{11}$  splitting can easily be determined either at  $B=0$  or by extrapolation of the  $2s$  transition energies for  $B \rightarrow 0$ . The exciton binding energy is then estimated by multiplying the  $2shh_{11}$ - $1shh_{11}$  splitting by a characteristic factor that depends critically on the dimension of the exciton. The characteristic factor is  $\frac{9}{8}$  for an ideal two-dimensional exciton, but it increases to  $\frac{4}{3}$  for an ideal three-dimensional exciton. Figure 4 shows the exciton binding energies obtained using differ-

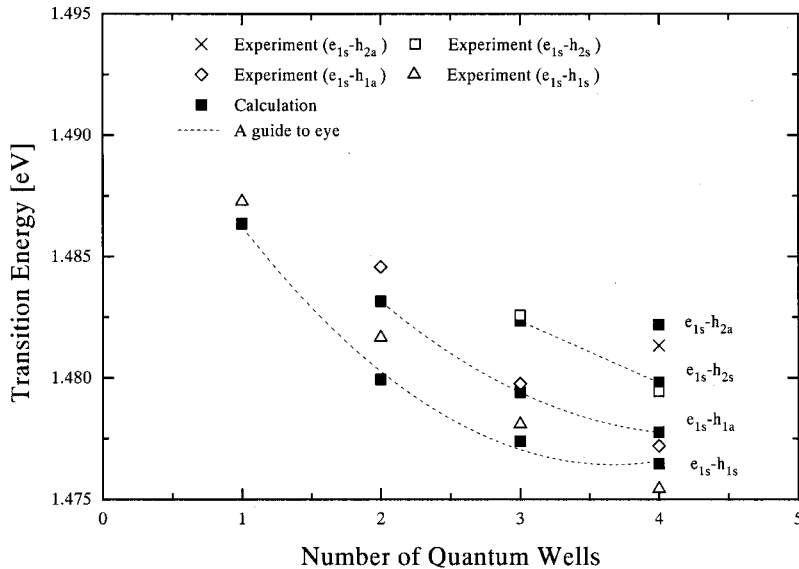


FIG. 3. Transition energy vs quantum-well number. The calculation is based on the single-particle model including the excitonic effect. Only the transitions associated with the  $e_{1s}$  state are given. The experimental results are from Fig. 1.

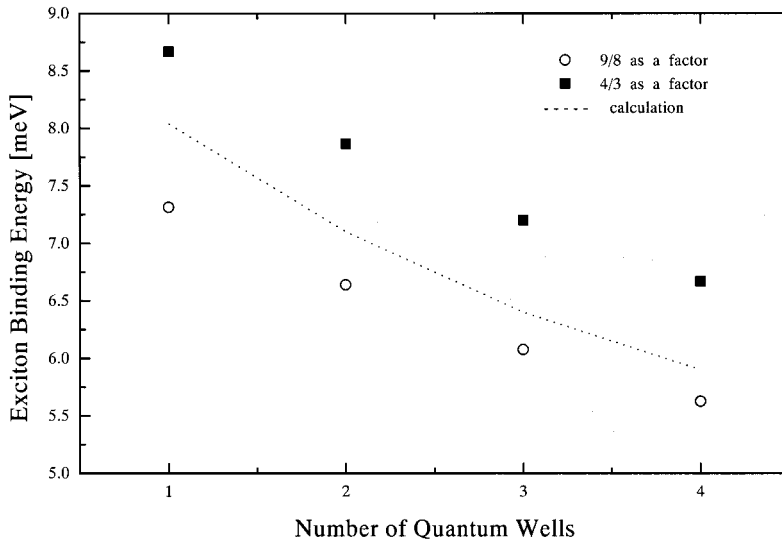


FIG. 4. The exciton binding energy versus quantum-well number for the calculation (dashed lines) and experimental results.  $\circ$  means the exciton binding energy was obtained using  $\frac{9}{8}$  as the characteristic factor,  $\blacksquare$  using  $\frac{4}{3}$ .

ent characteristic factors and the calculated exciton binding energies as a function of quantum-well number. The exciton binding energy decreases with increasing quantum-well number. By comparing the experimental and calculated results, the experimental result is found to be a little larger than the calculated result using  $\frac{4}{3}$  as the characteristic factor; and the situation is reversed if one uses  $\frac{9}{8}$  as the characteristic factor. This means that the excitons in these structures possess somewhat three-dimensional character due to the coupling. This is also clearly shown by the wave functions for the electron [Fig. 5(a)] and heavy hole [Fig. 5(b)] as a function of the coordinate  $z$  normal to the well planes.

### V. $hh_{21}$ AND $1lh$ EXCITON PROPERTIES

This section discusses the effect of strong mixing between heavy- and light-hole excitons on excitonic states in mag-

netic fields, in particular, the properties of forbidden transitions and light-hole excitons due to the strong mixing effect. In this case, the three-coupled-quantum-well structure (i.e.,  $i=3$ ) is used as the example. Figure 6 presents the PLE spectra of the  $i=3$  case in magnetic fields up to 13 T recorded in the  $\sigma^-$  polarization. The fan charts of the spectral lines obtained in the  $\sigma^+$  and  $\sigma^-$  polarizations are displayed in Figs. 7(a) and 7(b). Figure 6 does not show the  $1shh_{11}$  transition because its intensity is too high but the data for  $1shh_{11}$  are given in Fig. 7.

First, a brief description of the basic excitonic states is given.  $1shh_{11}$  and  $2shh_{11}$  excitonic states can easily be determined based on a detailed calculation and symmetry analysis. Both of these two states are of  $\Gamma_{7g}$  symmetry. When they approach each other, an anticrossing occurs between them.<sup>1</sup> Figure 6 shows a strong anticrossing effect in

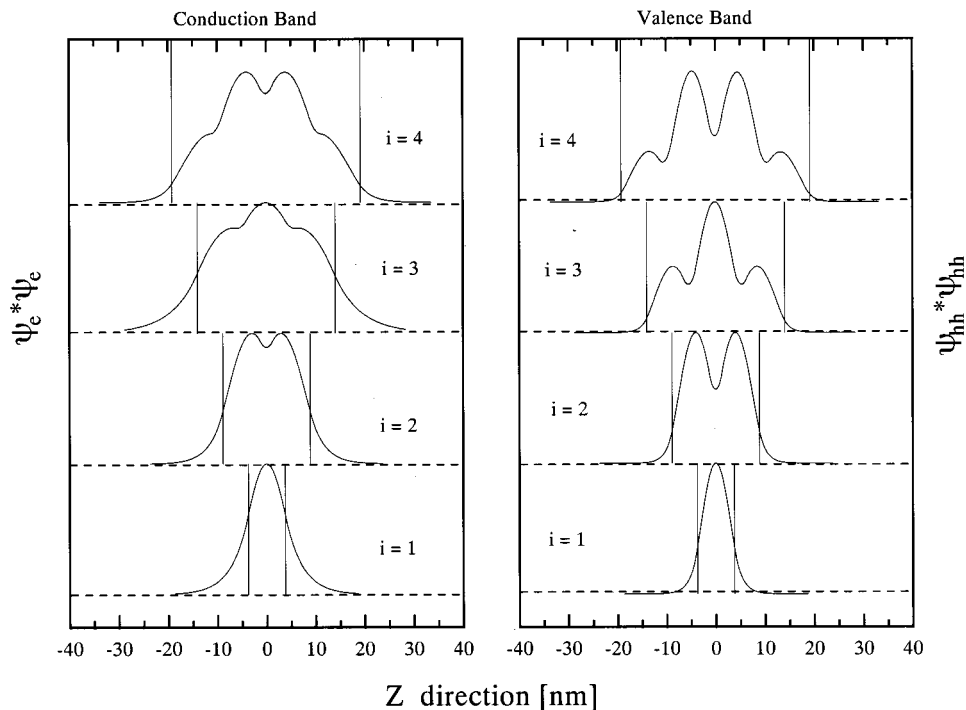


FIG. 5. Square of the electron (a) and heavy-hole (b) ground-state wave functions as a function of  $i$  (from bottom to top,  $i=1,2,3,4$ ).

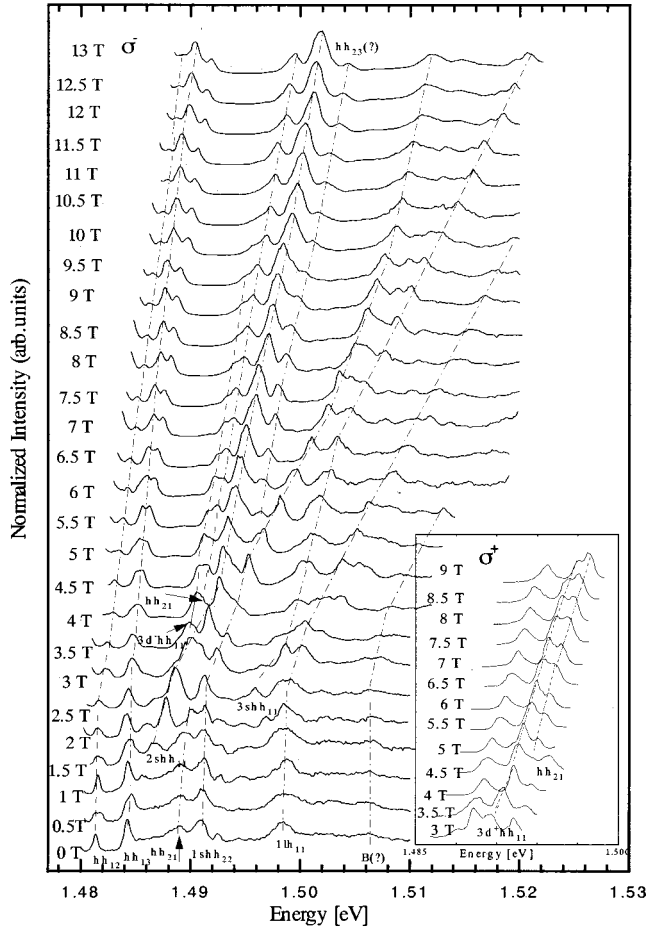


FIG. 6. PLE spectra of structures with  $i=3$  in magnetic fields up to 13 T in the  $\sigma^-$  polarization. The ground-state transition is not given. Inset gives the spectra in  $\sigma^+$  polarization.

the range between 2 and 4.5 T. The single-particle model including the excitonic effect is used to calculate the energy position. The calculation agrees well with experimental results at zero magnetic field as shown in Table I, in which the transition energies are given using the ground state  $E_{hh_{11}}$  as a reference. For the other basic excitonic transitions, such as  $hh_{12}$ ,  $hh_{13}$ , etc. Table I also gives the energy positions at zero magnetic field. Their identification can also be examined by analyzing their oscillator strength. Normally, the oscillator strength of a transition with even transition index  $\Delta n$  should be higher than that of a transition with odd  $\Delta n$ . At  $B=0$ , the intensity of  $hh_{13}$  is higher than that of  $hh_{12}$  and the intensity of  $1shh_{22}$  is higher than that of  $1lh_{21}$ .

The appearance of forbidden transitions is due to the mixing between heavy- and light-hole excitons. The  $hh_{12}$  exciton seems to be simple; here we would like to study the properties of the  $hh_{21}$  exciton depicted in Fig. 6 since there are only a few reports on it and also it has a strong interaction with other excitons at high magnetic fields. Before the discussion, we briefly describe the  $3dhh_{11}$  exciton since there is an interaction between them. Based on the calculation of Bauer and Ando,<sup>1</sup> the  $3d^-hh_{11}$  exciton transition should appear slightly below the  $2shh_{11}$  transition, while the energy of  $3d^+hh_{11}$  in the  $\sigma^+$  polarization should be higher than that of  $3d^-hh_{11}$  in the  $\sigma^-$  polarization. Comparing the spectra in the  $\sigma^+$  and  $\sigma^-$  polarizations, the  $3dhh_{11}$  exciton can easily be determined. It has  $\Gamma_{6g}$  symmetry.<sup>1</sup> The calculation of Bauer and Ando<sup>1</sup> predicted that the mixing between heavy- and light-hole excitons leads to the appearance of the  $hh_{21}$  exciton. The calculation of Chan<sup>5</sup> further indicated that the  $p$  exciton of  $hh_{21}$  is mixed with the  $s$ -symmetry exciton of  $1lh$ . Since both the  $p$  exciton of  $hh_{21}$  and the  $s$  exciton of  $1lh$  have  $\Gamma_{6g}$  symmetry,  $hh_{21}$  should appear with  $\Gamma_{6g}$  symmetry. Therefore, there should exist an anticrossing when  $3dhh_{11}$  approaches  $hh_{21}$ . In Fig. 6, between 2.5 and 4 T, the  $hh_{21}$  exciton is almost invisible since  $2shh_{11}$  is very close to it and

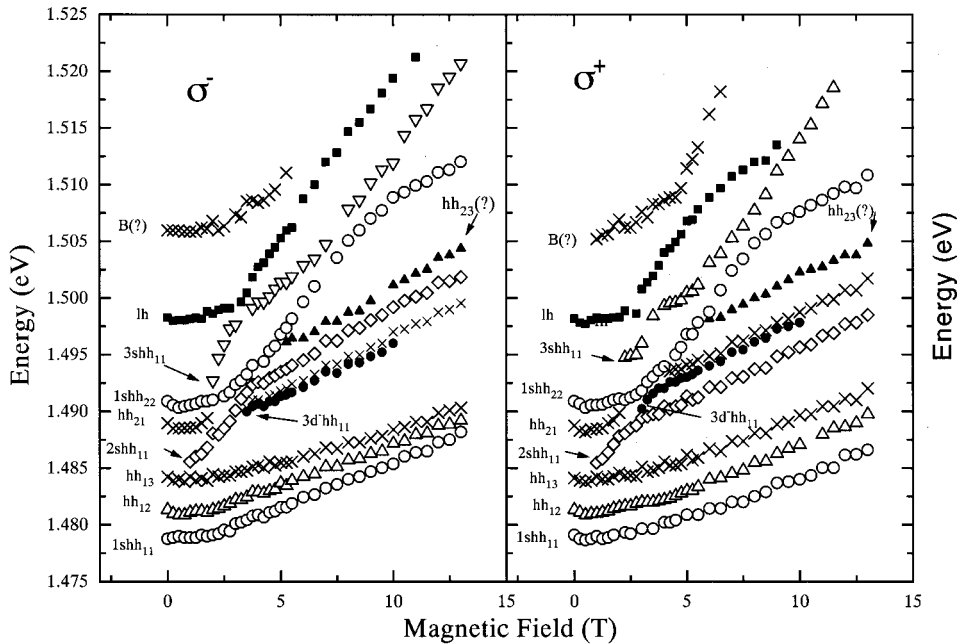


FIG. 7. Magnetic-field-dependent excitonic transitions in the  $\sigma^-$  (a) and  $\sigma^+$  (b) polarizations for the case of  $i=3$ .

TABLE I. The calculated and experimental results for exciton transition energies (meV) in the case of  $i=3$  with 9 ML GaAs separating the quantum wells.

	$E_{hh_{12}}-E_{hh_{11}}$	$E_{hh_{13}}-E_{hh_{11}}$	$E_{hh_{21}}-E_{hh_{11}}$	$E_{hh_{22}}-E_{hh_{11}}$	$E_{lh}-E_{hh_{11}}$
Experiment	2.57	5.48	10.2	12.12	19.51
Calculation	2.02	4.94	9.50	11.52	18.1 (Ref. 26)

the  $2shh_{11}$  intensity is greatly enhanced in this region. Beginning at 4 T,  $2shh_{11}$  is far from  $hh_{21}$ , and  $hh_{21}$  can easily be observed to appear slightly above  $3dhh_{11}$  in the  $\sigma^-$  polarization. (Similarly,  $hh_{21}$  appears above  $3d^+hh_{11}$  in the  $\sigma^+$  polarization.) Between 4 and 10 T, the intensity of the original  $3d^-hh_{11}$  exciton becomes weaker and weaker; finally, it is invisible, while the intensity of  $hh_{21}$  becomes stronger and stronger. Obviously, an anticrossing occurs between the  $3d^-hh_{11}$  and  $hh_{21}$  excitons. In fact, the anticrossing between  $3d^+hh_{11}$  and  $hh_{21}$  is shown more clearly in the  $\sigma^+$  polarization shown in the inset of Fig. 6. Since the  $3dhh_{11}$  exciton has  $\Gamma_{6g}$  symmetry, of course  $hh_{21}$  also possesses  $\Gamma_{6g}$  symmetry based on the theory of Bauer and Ando.<sup>1</sup> To our knowledge, this is the first report of the anticrossing between the  $3dhh_{11}$  and  $hh_{21}$  excitons.

The behavior of the 1lh exciton transition appearing at 1.4983 eV at zero magnetic field is rather complicated. Without heavy- and light-hole exciton mixing, it cannot be understood. Between 2.5 and 4.5 T, the 1lh exciton has an anticrossing with  $3shh_{11}$ . After this region, the original 1lh exciton is repelled to a high-energy position by  $3shh_{11}$  and the original  $3shh_{11}$  reaches the position of the 1lh, that is, they exchange properties. Between 6 and 10 T, the original  $3shh_{11}$  (now 1lh due to the anticrossing mentioned above) undergoes a second anticrossing with  $2shh_{11}$  which is changed from the original  $1shh_{22}$ . The second anticrossing is much stronger than the first, as can be seen from the variation of oscillator strength. After the anticrossing region, the original  $3shh_{11}$  (i.e., 1lh after the first anticrossing) and  $2shh_{11}$  exchange properties. The original  $3shh_{11}$  is repelled to a higher-energy position and its oscillator strength increases with increasing magnetic field; at the same time,  $2shh_{11}$  is repelled to the lower-energy position and its oscillator strength remains almost the same with increasing magnetic field. Comparing these two anticrossings, the repulsion is found to be strongly dependent on the value of the excited-

state index  $n$ , which is in good agreement with the calculation of Bauer and Ando<sup>1</sup> that the anticrossing effect decreases monotonically with  $n$ .

On the one hand, from the discussion above, 1lh possesses  $\Gamma_{7g}$  symmetry since it has an anticrossing with  $3shh_{11}$  ( $\Gamma_{7g}$  symmetry); on the other hand, the theory of Bauer Ando<sup>1</sup> indicates that the 1lh exciton ground state (i.e.,  $1sh$ ) should have  $\Gamma_{6g}$  symmetry. Since there exists a strong mixing between heavy- and light-hole excitons, 1lh in our case should contain some component from the heavy hole with  $\Gamma_{7g}$  symmetry, which results in an anticrossing with  $3shh_{11}$ . Therefore, the light-hole exciton in our case possesses  $\Gamma_{6g}$  and  $\Gamma_{7g}$  symmetry; this effect should be considered in analyzing other complicated excitonic states in future.

## VI. SUMMARY

In summary, a study of excitonic states has been carried out in  $\text{In}_{0.045}\text{Ga}_{0.955}\text{As}/\text{GaAs}$  coupled quantum-well structures consisting of  $i=1,2,3,4$  quantum wells. Because of the coupling of  $i$  quantum wells, the heavy-hole state of each separate quantum well is split into  $i^2$  states. Study of the binding energy of the ground-state exciton shows that these coupled quantum-well structures are neither of ideal two-dimensional nor of ideal three-dimensional form. Increasing quantum-well number, which results in a decrease of exciton binding energy, enhances this effect.

Highly resolved PLE spectra of three-coupled-quantum-well structures are presented in magnetic fields  $B \leq 13$  T. An anticrossing is observed to occur between  $hh_{21}$  and  $3dhh_{11}$ , and the light hole is found to possess both  $\Gamma_{7g}$  and  $\Gamma_{6g}$  symmetry.

## ACKNOWLEDGMENT

One of the authors (T.W.) would like to thank the Volkswagen Foundation for financial support.

\*Corresponding author: Satellite Venture-Business Laboratory, Department of Electrical and Electronic Engineering, University of Tokushima, Tokushima 770-8506, Japan.

<sup>1</sup>G. E. W. Bauer and T. Ando, Phys. Rev. B **38**, 6015 (1988).

<sup>2</sup>G. E. W. Bauer and T. Ando, Phys. Rev. B **37**, 3130 (1988).

<sup>3</sup>L. Viña, R. T. Collins, E. E. Mendez, and W. I. Wang, Phys. Rev. Lett. **58**, 832 (1987).

<sup>4</sup>L. Viña, G. E. W. Bauer, M. Potemski, J. C. Maan, E. E. Mendez, and W. I. Wang, Phys. Rev. B **41**, 10 767 (1990).

<sup>5</sup>K. S. Chan, J. Phys. C **19**, L125 (1986).

<sup>6</sup>I. Galbraith and G. Duggan, Phys. Rev. B **40**, 5515 (1989).

<sup>7</sup>A. B. Dzyubenko and A. L. Yablonski, Phys. Rev. B **53**, 16 355 (1996).

<sup>8</sup>L. Butov, A. Zrenner, G. Abstreiter, G. Böhm, and G. Weimann, Phys. Rev. Lett. **73**, 304 (1994).

<sup>9</sup>T. Fukuzawa, E. E. Mendez, and J. M. Hong, Phys. Rev. Lett. **64**, 3066 (1994).

<sup>10</sup>M. Bayer, V. B. Timofeev, F. Faller, T. Gutbrod, and A. Forchel, Phys. Rev. B **54**, 8799 (1996).

<sup>11</sup>L. Butov, A. Zrenner, G. Abstreiter, A. V. Petinova, and K. Eberl, Phys. Rev. B **52**, 12 153 (1994).

<sup>12</sup>T. Westgaard, Q. X. Zhao, B. O. Fimland, K. Johannessen, and L. Johnsen, Phys. Rev. B **45**, 1784 (1992).

<sup>13</sup>V. D. Kulakovskii, A. Forchel, K. Pieger, J. Straka, B. N. Shepel, and S. V. Nochevny, Phys. Rev. B **50**, 7467 (1994).

<sup>14</sup>S.-R. Eric Yang and L. J. Sham, Phys. Rev. Lett. **58**, 2598 (1987).

<sup>15</sup>D. C. Rogers, J. Singleton, R. J. Nicholas, C. T. Foxon, and K. Woodbridge, Phys. Rev. B **34**, 4002 (1986).

<sup>16</sup>K. J. Moore, G. Duggan, K. Woodbridge, and C. Roberts, Phys. Rev. B **41**, 1095 (1990).

- <sup>17</sup>K. J. Moore, G. Duggan, A. Raukema, and K. Woodbridge, Phys. Rev. B **42**, 1326 (1990).
- <sup>18</sup>K. J. Moore, G. Duggan, K. Woodbridge, and C. Roberts, Phys. Rev. B **41**, 1090 (1990).
- <sup>19</sup>L. W. Molenkamp, G. E. W. Bauer, R. Eppenga, and C. T. Foxon, Phys. Rev. B **38**, 6147 (1988).
- <sup>20</sup>M. M. Dignam and J. E. Sipe, Phys. Rev. B **43**, 4084 (1991).
- <sup>21</sup>T. Yasui, Y. Segawa, Y. Aoyagi, Y. Iimura, G. E. W. Bauer, I. Mogi, and G. Kido, Phys. Rev. B **51**, 9813 (1995).
- <sup>22</sup>M. Potemski, L. Viña, G. E. W. Bauer, J. C. Maan, K. Ploog, and G. Weimann, Phys. Rev. B **43**, 14 707 (1991).
- <sup>23</sup>R. C. Miller, A. C. Gossard, G. D. Sander, Yia-Chung Chang, and J. N. Schulman, Phys. Rev. B **32**, 8452 (1985).
- <sup>24</sup>R. J. Warburton, R. J. Nicholas, S. Sasaki, N. Miura, and K. Woodbridge, Phys. Rev. B **48**, 12 323 (1993).
- <sup>25</sup>T. Wang, M. Bayer, and A. Forchel, Phys. Rev. B **58**, R10 183 (1998).
- <sup>26</sup>It is assumed that the exciton binding energies for the heavy-hole excitons are the same and about 6.1 meV in the calculation (seen in Fig. 4). Since the light-hole state in the valence band is unconfined, for simplicity, the light-hole exciton binding energy can be thought to have the same value as in the 3D case. The binding energy of the light-hole exciton can be estimated by comparing the effective masses of heavy- and light-hole excitons. For 3D GaAs, the heavy-hole exciton binding energy is about 4 meV (Ref. 27). The binding energy of the light-hole exciton is about 2.6 meV.
- <sup>27</sup>C. F. Kinghirn, *Semiconductor Optics* (Springer-Verlag, Berlin, 1995), p. 166.